Proceedings of the XVIII International Symposium on Dynamic Problems of Mechanics (DINAME 2019),
M.A. Savi, T.G. Ritto and W.M. Bessa (editors), ABCM, Buzios, RJ, Brazil, March 10th to 15th, 2019

Fuzzy inference of oil furnace combustion state through computer vision information

Gustavo C. S. Neto (gustavoneto@usp.br)[1], Danilo S. Chui (danilochui@usp.br)[1], Flavio C. Trigo (trigo.flavio@usp.br)[1], Flavius P. R. Martins (flavius.martins@usp.br)[1] and Agenor T. Fleury (agenorfleury@usp.br)[1]

[1] Universidade de São Paulo, Escola Politécnica, Av. Prof. Mello Moraes 2231, 05508-930 São Paulo, SP, Brazil

Abstract: Regular furnace operation systems require continuous monitoring of air/fuel ratio, oil and water temperatures, combustion byproducts emissions, etc. Experts analyze these data to detect anomalies and act to prevent the system to reach critical or undesired conditions. PID controllers may control parameter reference levels, however human decision is still crucial to the control process. A first step on human decision is to recognize flame patterns that constitute anomalous behavior and then, through experience, change parameters to stabilize the combustion process. This research focus on this first step and proposes a method that infers different anomalous states from images captured by a digital camera from an experimental oil furnace. Different image processing algorithms extract information through features vectors that are analyzed by a previously trained "artificial expert". State of the combustion processes are then obtained through fuzzy inference together with estimated input values. Results show that the proposed "artificial expert" is able identify most different anomalous states as desired.

Keywords: combustion diagnostics, digital image processing, fuzzy inference

INTRODUCTION

Industrial furnace operation requires an extensive network of sensors and safety measures to assure a continuous and stable combustion process. Even though sophisticated supervisory systems may provide several pieces of information and control systems are available for reference tracking parameters, e.g., PID controllers, there are a great number of factors that can cause deviations from optimal combustion operation. For such cases, human experts still play a fundamental role on decision making, due to their accumulated technical experience and their pattern recognition ability.

Combustion processes inside furnace chambers are subjected to a variety of physical phenomena, such as acoustic vibrations inside the chamber, heat transfer between the flame and the surroundings, interaction of fluids with different velocities that suffer chemical reactions, and so on. This complexity poses a great difficulty on modeling the combustion process. Thus, creating supervisory or control systems that can predict combustion state or correct possible deviations is a very challenging task, making the job of technical experts even more relevant for this application.

On the other hand, several researches try to overcome modeling difficulties and attempt to mimic the human decision making process (Li and Chang, 2000; Cho et al., 1998). González-Cencerrado, Peña and Gil (2012) studied the influence of the air-fuel ratio on the structure and stability of the flame from images obtained by a CCD camera in a swirl-stabilized, semi-industrial scale burner of 500 kW_{th} for biomass processing with pulverized coal. Chen, Chan and Cheng (2013) used flame images along with principal component analysis for modeling the combustion in a heavy oil burner. From a set of 300 colored images (RGB standard), a matrix was assembled in which each line is formed by three ordered vector blocks containing the red, green and blue tones of an image. That is, for an RGB image of 658×492 , each line will have dimension of $3 \cdot 658 \cdot 492$. With this matrix, it was found that the first two components presents 98.8% of the total variance of flame image. Tóth et al. (2017) investigated the use of deep belief networks using routinely measured operational parameters and real-time flame imaging to predict the thermal output of a 3 MW biomass boiler. It was found that flame images analysis increases the accuracy of predictions compared to those obtained using only operational data. Sreedhanya et al. (2017) used the Mamdani inference method (Mamdani and Assilian, 1975) to estimate the temperature measurement based on the red, green and blue tones of the flame image of a typical rotary kiln of the cement manufacturing process.

An indicator that the combustion process in furnaces is according to specifications is the stability of its flame. It should be monitored and maintained continuously to improve overall combustion performance. Stability depends on a number of factors, such as fuel type, equivalence ratio, furnace structure and type of burner. Since flame stability is closely linked to the combustion efficiency and its respective pollutant emissions, several techniques for flame monitoring and characterization have been proposed. Bertucco et al. (2000), which presents the proposal of an approach by cellular neural networks for real-time analysis in the combustion process of a garbage incinerator. Fleury, Martins and Trigo (2009) propose an approach for the monitoring of oil furnace flames by identifying the quality of nebulization using computer vision and Kalman filter techniques. In this work, they used CCD video cameras sensitive to the infrared spectrum to

capture and monitor the flame rather than conventional sensors. From the capture of these images, properties such as brightness, geometry and spectrum of spatial frequencies are used to construct a vector of characteristics, considered the state of the dynamic system. Estimates of this vector, whose model of propagation adopted is the random walk, are obtained with a Kalman filter.

Fleury, Trigo and Martins (2013) proposed an estimation method for atomization quality from grabbed flame images on an industrial furnace that burns fuel oil type 1. They classified flame atomization quality based on a fuzzy rule, and then estimated quality of new flames combining a random-walk model with Kalman filtering. This research triggered a series of articles that related flame images processed by computer vision techniques to aspects of the combustion process dynamics (Silva et al., 2015; Fleury et al., 2015). Recently, Fleury et al. (2018) proposed an inference model to correlate 33 flame image features with 5 physical input values, that could make combustion state diagnostics among 9 flame state categories. That inference engine, based on Dempster-Shafer method, was able to recognize most of the sudden changes in the combustion process resulting from the modification of physical parameters.

This work makes further developments on the results of Fleury et al. (2018) for the same objective that is to correlate input physical data to flame image features and classify different flame states as flame categories. Instead of using Dempster-Shafer method, a fuzzy inference engine based on 11 image features will correlate 3 physical input values, and in addition to classify the flame image into 5 flame state categories, it will also estimate input values for each flame image.

EXPERIMENTAL EQUIPMENT

Experimental data were obtained from a vertical furnace with 4.0 m height and 1.5 m internal diameter, that is divided in 12 water cooled ring blocks. The burner, located at the bottom, presents two manually controlled air inlets for primary and secondary air supplies, as shown on Fig. 1, and may process up to 80 kg/h of fuel oil number 1. At the top, an opening leads the combustion byproduct gases to the exhaust pipe. A digital camera especially prepared for high temperature applications is placed at the central cross-section block of the furnace. It has a heat shield and a water cooling system to allow continuous operation in the hostile environment of the working furnace.

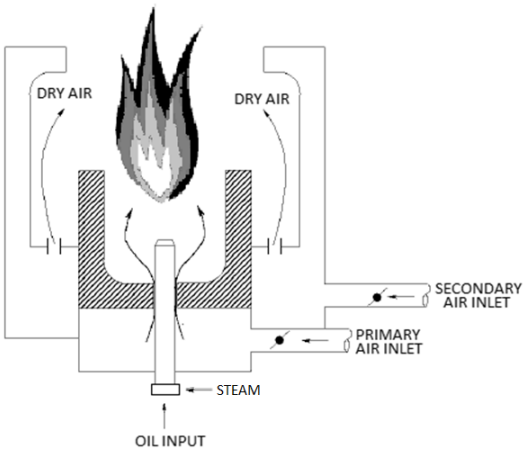

Figure 1 – Burner schematics, adapted from Fleury et al. (2013).

Images of the combustion process were captured by a monochromatic RS-170 CCD camera coupled with a narrow band-pass interferometric filter at 900 nm wave length, which is the range of the radiation of the soot that corresponds to almost all the radiation emitted by a typical oil flame, mounted over a 6 mm lens (f/1.2). Video data acquisition was made through a frame grabber board at sampling rate of 25 Hz, whose output were interlaced 640 x 480 pixel images. In order to correlate flame images to physical variables, other process parameters needed to be monitored: fuel pressure, mass flow and temperature, nebulization steam pressure, flow and temperature, exhaust gases temperature and concentration of CO, CO_2, SO_2, O_2 and NO_x.

FLAME CLASSIFICATION AND IMAGE ANALYSIS

Three input variables were selected as effective on acting over the system response: SFR (steam to fuel ratio), EA (% excess air) and PSAFR (primary to secondary air flow ratio). Steam to fuel ratio is a measure of atomization of the fuel and affects consumption and combustion quality. Additionally, the excess air measures how fuel poor the mixture is, and have great influence over the exhaust gas emissions. And also, primary to secondary air flow ratio affects the stability of the flame. A design of experiments was carried out to analyze the influence of each of three input variables in the most

separate way as possible. Each experimental run with different input values were named as a "Parameter Set". Groups of parameter sets were classified according to the opinion of an expert into different categories of flame. Figure 2 shows examples of segmented images of each category and contents of Tab. 1 sum up the information of the tests.

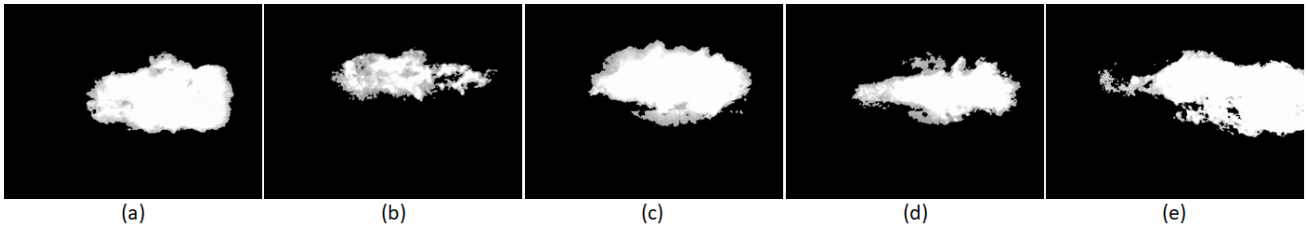

Figure 2 – (a) Stable flame. (b) Unstable flame. (c) Low excess air flame. (d) High excess air flame. (e) Poorly atomized flame

Table 1 – Experimental operational parameters by flame category.

Category	Parameter Set	Primary air flow (m^3/h)	Secondary air flow (m^3/h)	Steam flow (kg/h)	Oil fuel flow (kg/h)	PSAFR	EA (%)	SFR
Stable, well-atomized and normal excess air	Nominal	500	500	23	70	1.00	3.0	0.33
	EA high level 1	500	500	23	70	1.00	3.8	0.33
	PSAFR high level 1	600	400	23	70	1.50	3.0	0.33
	PSAFR high level 2	650	350	23	70	1.86	3.0	0.33
	SFR high level 1	500	500	25	70	1.00	3.0	0.36
	SFR high level 2	500	500	30	70	1.00	3.0	0.43
	SFR high level 3	500	500	35	70	1.00	3.0	0.50
	SFR high level 4	500	500	40	70	1.00	3.0	0.57
Unstable	PSAFR high level 3	700	300	23	70	2.33	3.0	0.33
Low excess air	EA low level 1	500	500	23	70	1.00	1.0	0.33
	EA low level 2	500	500	23	70	1.00	1.5	0.33
High excess air	EA high level 2	500	500	23	70	1.00	5.0	0.33
	EA high level 3	500	500	23	70	1.00	6.0	0.33
Poorly atomized	SFR low level 1	500	500	20	70	1.00	3.0	0.29
	SFR low level 2	500	500	18	70	1.00	3.0	0.26
	SFR low level 3	500	500	16	70	1.00	3.0	0.23
	SFR low level 4	500	500	15	70	1.00	3.0	0.21
	SFR low level 5	500	500	12	70	1.00	3.0	0.17

Flame Image Processing

From experimental data, image sequences were obtained for each "Parameter Set" of Tab. 1. As the acquisition module delivers interlaced images, the first step is to deinterlace them. Deinterlacement process generates two non-interlaced images called odd and even images, which is a reference to the line numbers from the original image. An original image from the "Nominal" parameter set and its deinterlaced counterparts are shown in Fig. 3(a) to 3(c).

Then, it is needed to separate the flame from the background of the furnace. A binarization process based on 1D Otsu method is used, Fig. 4(b). After that, segmentation is completed using the white part of the binarized image as a filter of the deinterlaced image, Fig. 4(c). Both binary and segmented image are used to form the respective feature vector.

Image Feature Vector

It is a common practice on image based classification problems to represent the image as a series of distinctive visual features or image characteristics. These data that summarize the image itself are gathered inside a feature vector. On a dynamic state identification of the flames, the calculation of such features and generation of these image vectors are continuous. For the identification of the flame state, it was used a group of 11 image features: f_1: Luminous region or simply the area of the binary image; f_2 and f_3: x and y coordinates of image centroid; f_4 and f_5: second moments of area relative to x and y axis; f_6: perimeter of the binary image; f_7: detachment from the burner, that is the closest distance from

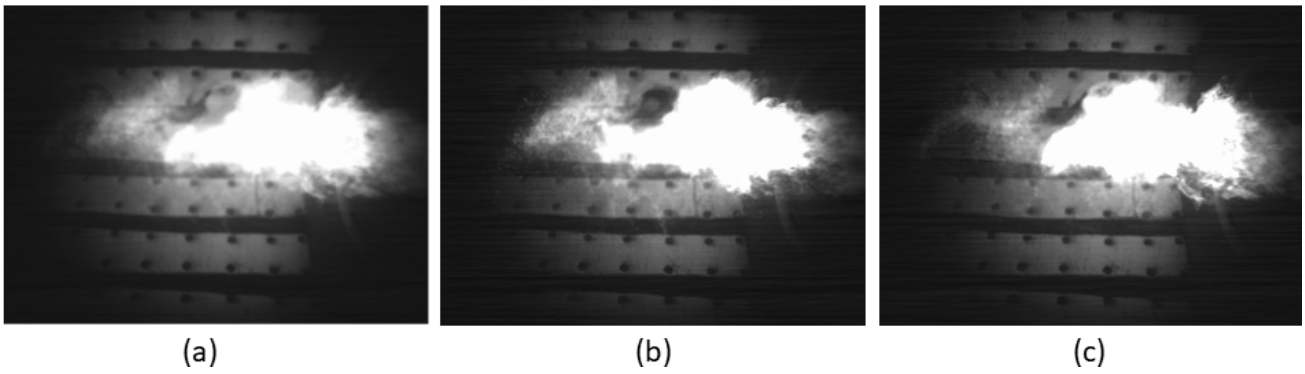

Figure 3 – (a) Original image. (b) Deinterlaced odd image. (c) Deinterlaced even image.

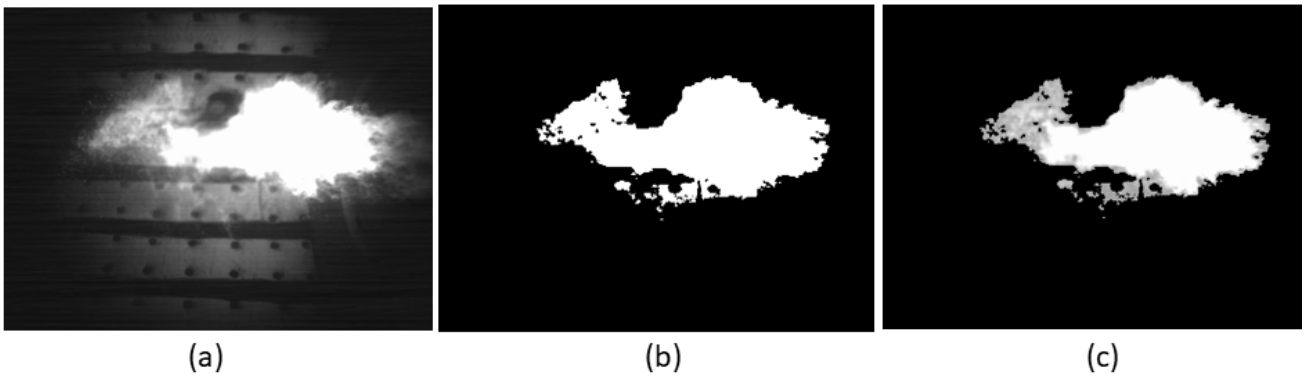

Figure 4 – (a) Deinterlaced even image. (b) Binarized image. (c) Segmented image

the burner location (or extreme right of the image) to the rightmost pixel of the image; f_8: dispersion, that is a measure of how clustered the pixels are, normalized by the area; f_9: eccentricity of an ellipse that approximately surrounds the image, maintaining an area that is approximately the area of the image; f_{10}: normalized average brightness of the image and f_{11}: non-uniformity, that is a measure of the deviation from the average brightness.

Available images from all the parameter sets were divided in the following manner: 70% for a training set to generate the fuzzy rules, and 30% for the validation set. Validation set data were used to test if the rules created with the training set lead to appropriate identification.

FUZZY INFERENCE

In most mathematically modeled phenomena, inaccurate data arises, often approximated by real numbers, which causes a certain "stiffness" in the model, often unnecessary. The Fuzzy Set Theory, introduced by Zadeh (1965), appears as an excellent alternative for modeling these problems. This fact leads to greater fidelity in the storage and processing of inaccurate concepts in computer programming, making operation with numbers that contain incorporated uncertainties possible.

A fuzzy set N of a classical set U, denominated universe of discourse, ($N \subset U$) is characterized by the function $\mu_N(x) : U \longrightarrow [0,1]$ so-called membership function of fuzzy set N. It is common to write the set N as a classical set formed by ordered pairs $N = \{(x, \mu_N(x))/x \in U\}$. That is, a fuzzy set is fully characterized by $\mu_N(x)$ and it represents the grade of membership of x in N. They map the elements of an universe set U to the interval $[0,1]$ and allow to specify how well an object satisfies a vague description. Thus, a sentence may be partially true and partially false.

A 4-tuple $[a\ b\ c\ d]$, with $a,b,c,d \in \mathbb{R}$, where "a" represents the smallest likely value, $[b,c]$ interval the most probable values, "c" the largest possible value of any fuzzy event and whose membership function's graph forms a trapezium is called Trapezoidal Fuzzy Number (TpFN). An example of this number is Fig.5. A particular case of TpFN is Triangular Fuzzy Number, where $b = c$, and it is denoted by $[a\ b\ d]$.

Fuzzy rules tend to mimic human behavior to infer an output based on input variables. A fuzzy rule may be written as *If* situation *Then* conclusion (*If* x is A *Then* y is B). The situation called rule antecedent, is defined as a combination of relations such as x *is* A for each component of a input vector. The conclusion part, y is B, is called consequence. Prade

and Dubois (1996) comment that *If / then* rules provide a suitable format for expressing parts of knowledge, but it is just a format which to cover different intended semantics and uses. A Fuzzy Inference System (FIS) is a manner of mapping an input space to an output space using *If / then* rules. A FIS tries to formalize the reasoning process of human language by terms of fuzzy logic (Barros and Bassanezi, 2010). In the flame identification problem, for each image acquired from the system, the state of the flame is inferred from image feature values.

In general, a FIS consists of following parts: i) *fuzzification module*, that transforms the inputs, which are generally measures (real numbers which are also called *crisp* numbers), into fuzzy sets. ii) *knowledge base*, which consists of a set of *If / then* rules supplied by specialists or prior informations. iii) *inference engine*, which simulates the human reasoning process by making fuzzy inference on the inputs and *If / then* rules and finally, iv) *defuzzification module*, which transforms the fuzzy set obtained by the inference engine into a crisp value. In this paper, the inference method to be used is the Mamdani fuzzy inference (Mamdani and Assilian, 1975), which is the most commonly seen fuzzy methodology due to its simple structure of "min-max" operations and was among the first control systems built using fuzzy set theory. Further information on the Mamdani's method can be found, for example, in Barros and Bassanezi (2010) and Mamdani and Assilian (1975).

Feature vector $f = [f_1 \cdots f_{11}]^T$ was created for all images of each category of the training set. This information together with the help of a specialist were used to create the linguistic variables of the fuzzification module, as well as its pertinence functions, which will form the antecedent of the rule base. For example, in the case of dispersion (f_8), it was created the partitions *low, medium, high* and *very high* by means of triangular and trapezoidal numbers obtained from minimum and maximum values of training images. Fig. 5 shows the membership functions of the dispersion feature. Fuzzy variable

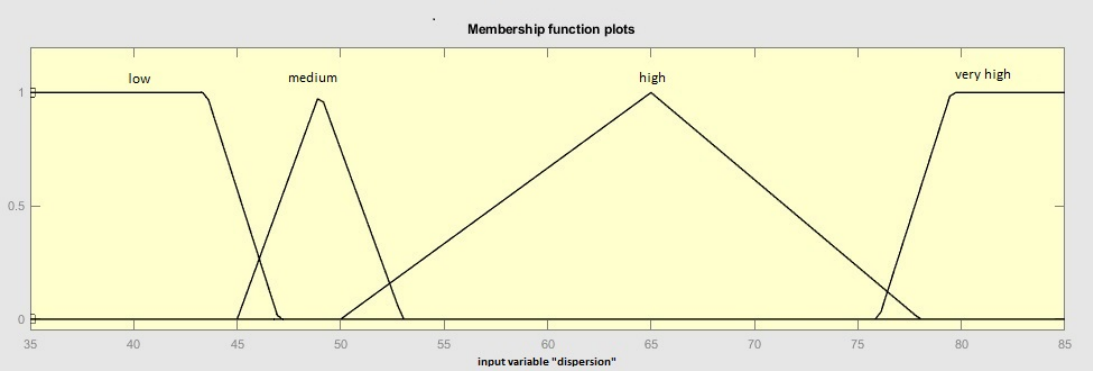

Figure 5 – Dispersion membership functions

outputs were designated according Tab. 1. Some parameter sets were grouped into the same output in order to reduce the number of rules in the inference module. For the SFR output, for instance, membership functions were created through triangular and trapezoidal numbers, setting the membership value 1 to the SFR value of the category indicated in Tab.1, which is the representative value of the class. Then, in case of SFR, the following linguistic variables were created:

- SFR normal: [0.28 0.33 0.35], that is, the value 0.33 has membership 1 to this set;
- SFR very low: [0.1 0.1 0.17 0.2], that corresponds to SFR low level 5;
- SFR low: [0.17 0.29 0.3], gathering SFR low level 1, 2, 3 and 4;
- SFR medium high: [0.33 0.36 0.4], that represents SFR high level 1;
- SFR high: [0.37 0.43 0.5], that represents SFR high level 2;
- SFR very high: [0.47 0.5 0.6 0.6], gathering SFR high level 3 and 4.

It is worth remembering that the representation [a b c] and [a b c d] in brackets refers to the triangular and trapezoidal fuzzy numbers, respectively. Fig.6 presents the membership functions of SFR. The same strategy was used to assemble the rule base: based on the spectrum of values obtained for the features of the training images and with the aid of a combustion specialist, 3172 rules were created for the inference engine. With these considerations, the fuzzy inference system was then assembled having as inputs the 11 fuzzified features of the images and as output the fuzzy numbers PSAR, SFR and EA.

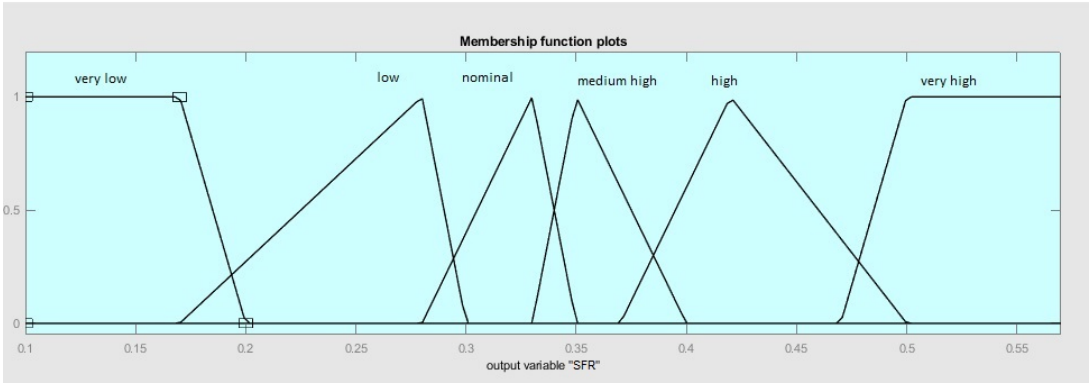

Figure 6 – SFR membership functions

RESULTS

Simulation results of validation tests made with obtained FIS are presented on Tab. 2. In these simulations the validation set of images were used for all the specified known conditions already shown on Tab. 1, processed through Fuzzy inference and classified into a *a priori* known category. Percentage of correct inference is obtained through a comparison between the known conditions of the experimental data and the inferred category for each image.

Table 2 – Results of FIS.

Category	Percentage of Correct Answers
Stable, Well-atomized and Normal Excess Air	95.45%
Unstable	83.33%
Poorly Atomized	97.96%
Low Excess Air	0.00%
High Excess Air	2.08%

From Tab. 2, it can be verified that for the analysis of flame instability, represented here by the imbalance of the primary and secondary air ratio (PSAFR), the FIS has a quite good percentage of correctness. In the case of wrongly inferred unstable flames, 16.67% may represent images that show a mixed behavior of stable and unstable conditions, and consequently their image features, although unstable, could be interpreted as a stable flame. Figure 7 shows the inferred values of PSAFR and EA and their target values for unstable flames. In this case, inferred values are close to the target values, with EA average a little greater than target value, but overall explain good performance on flame classification.

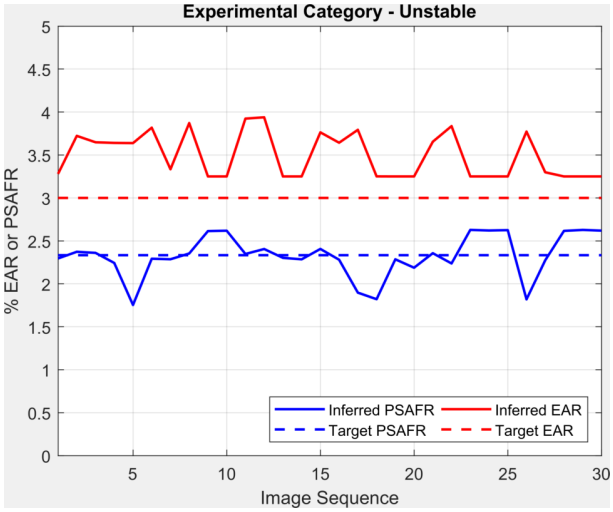

Figure 7 – Inferred PSAFR and EA values vs. target values for unstable flames

A better performance were observed for “Stable, Well-atomized and Normal Excess Air” and “Poorly Atomized” categories with errors of only 4.55% and 2.04%, respectively. Figure 8 shows he inferred values of PSAFR and EA and their target values for stable, well atomized and with normal excess air flames. It can be seen that, although some of punctual disparities exist, inferred values tend to follow target values.

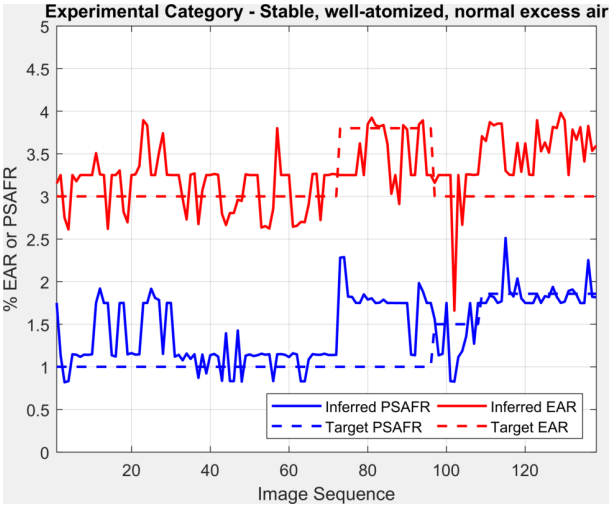

Figure 8 – Inferred PSAFR and EA values vs. target values for stable, well atomized and with normal excess air flames

In the “Low Excess Air” and “High Excess Air” cases, the designed FIS presented a poor outcome. This is due to the fact that FIS is in doubt between a Normal Excess Air flame and its correct category. In most cases, this is due to the fact that the highest membership is from the Normal Excess Air category, then the classification of the validation data indicates that there is no combustion irregularity. It should be noted that the FIS makes no confusion between High and Low Excess Air. High Excess Air images were classified either as Normal or High Excess Air. On the other hand, Low Excess Air images were all classified as Normal Excess Air. This indicates that it may be necessary to add other indicators to help FIS distinguish flames with Normal Excess Air from flames with disturbances in Excess Air, either low or high. Figure 9 shows a comparison of either low and high excess air cases for their inferred and target EA values. For both cases, inferred values have average values close to 3%, which is the nominal value for the EA variable. Thus, it can be seen that designed FIS is not evaluating EA properly, as discussed above.

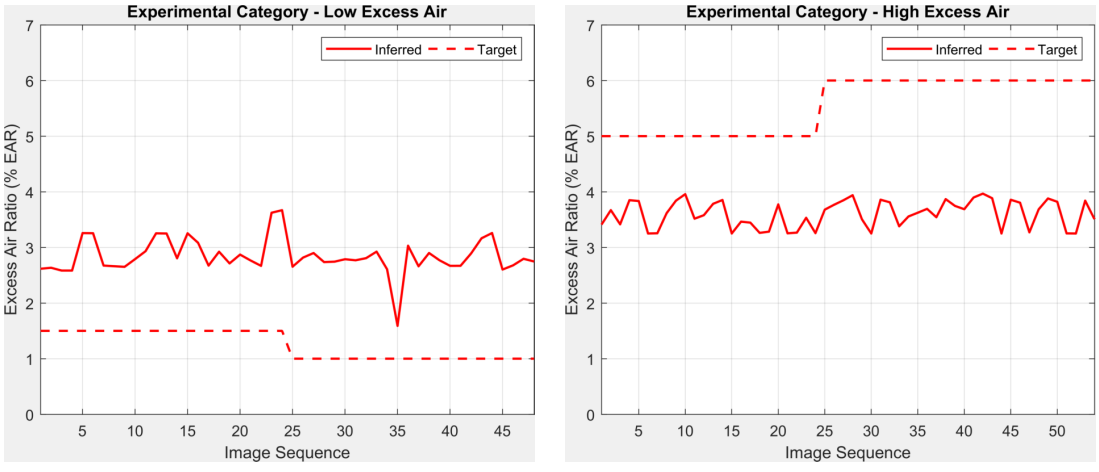

(a) (b)

Figure 9 – Inferred EA values vs. target values for (a) low excess air and (b) high excess air cases

In order to verify the behavior of the inference engine on a dynamic situation, a simulation was carried out gradually varying input PSAFR. Inference engine maintains its state identification with few deviations to the desired state according to the right categories. Figure 10 shows the evolution membership values throughout the image sequence. From image 1

to 82, parameter sets change from Nominal to PSAFR high level 1 and then to PSAFR high level 2, all of them composing the category "Stable, well-atomized and normal excess air". Even though, the inference identifies conditions PSAFR high level 1 and PSAFR high level 2 as Nominal, all these parameter sets fall into the same category, due to similarity on flame responses. From image 83 to 111, inference engine presents some difficulty on locking the identification to PSAFR high level 3, but most of the samples were identified as "Unstable", due to a larger membership for PSAFR high level 3, as showed on Tab. 2.

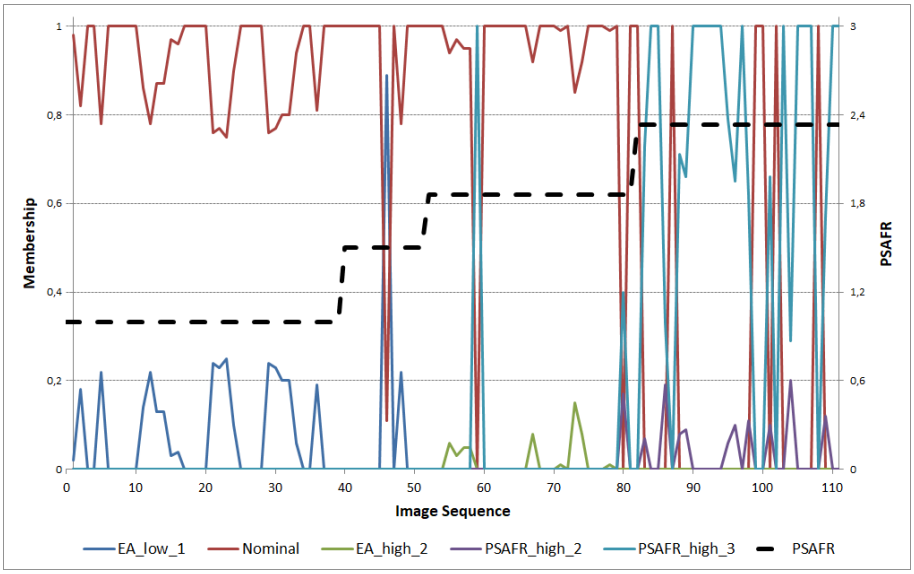

Figure 10 – State inference for sequence of images for PSAFR variation

CONCLUSIONS

In this paper, the objective was to obtain an intelligent framework that identifies some types of anomalies in oil furnace combustion processes and to infer values related to important indicators on combustion quality, namely SFR, EA and PSAFR from images obtained from a CCD camera. In order to train the artificial intelligence, tests under conditions known *a priori* were made and their images classified by a specialist. These images were processed in the search for features that translated the behavior of these combustion conditions. These features were used together with the expert's knowledge to obtain the fuzzification module and the inference engine for the fuzzy inference system (FIS). After that, validation tests were done in order to verify the accuracy of the FIS. The results showed that this inference machine presents good results for detection of atomization defects (related to SFR variable) and instability in the primary/secondary air ratio (related to PSAFR variable). For the imbalance in excess air, the system has difficulty on distinguishing among flames with normal excess air and altered excess air, indicating the need of embedding different types of information to the inference engine, and it will require further research to overcome this problem. However, it should be noted that although excess air anomalies were not identified correctly, the inference engine does not confuses low excess air with high excess air, and vice-versa, which is good news if one supposedly design a controller, for it would not act against the actual anomaly to bring it to nominal condition. In any case, the proposed model presents itself as a tool for detecting and inferring indicators of atomization defects and imbalance in the primary/secondary air ratio, and also gives an estimation of quantitative value for these variables.

ACKNOWLEDGMENTS

Danilo Chui is being granted with a scholarship support from FAPEAM, through the RH-DOUTORADO program.

Gustavo Neto acknowledges to FAPEAM/CAPES by the scholarship support, through the PROPG program.

The authors want to express their gratitude to Fausto Furnari for his invaluable technical support.

REFERENCES

Barros, L. C.; Bassanezi, R. C. "Tópicos de lógica fuzzy e biomatemática". Biomathematics Group, Institute of Mathematics, Statistics and Scientific Computation (IMECC), Campinas State University (UNICAMP), 2010.

Chen, J., Chan, L.L, and Cheng, Y., 2013, "Gaussian process regression based optimal design of combustion systems using flame images". Applied energy, Vol.111, pp. 153-160.

Bertucco, L., Fichera, A., Nunnari, G., & Pagano, A. ,2000, " A cellular neural networks approach to flame image analysis for combustion monitoring". In Cellular Neural Networks and Their Applications (CNNA 2000). Proceedings of the 6th IEEE International Workshop on (pp. 455-459). IEEE.

Cho, W. S., Ro, S. D., Kim, S. W., Jang, W. H., Shon, S. S., 1998, "The process modelling and simulations for the fault diagnosis of rotary kiln incinerator process", Journal of Industrial and Engineering Chemistry, 4, pp. 99104.

Fleury, A. T.; Trigo, F. C.; Martins, F. P. R. , 2009, "Application of Computer Vision and Kalman Filtering Techniques to Identify Oil Flames Nebulization Quality". In: 20th International Congress of Mechanical Engineering. Gramado-RS-Brazil. 2009.

Fleury, A.T., Trigo, F.C., Martins, F.P.R., 2013, "A new approach based on computer vision and nonlinear Kalman filtering to monitor the nebulization quality of oil flames", Elsevier-Expert Systems with Applications, Vol. 40, N. 12, pp. 4760-4769.

Fleury, A.T., Chui, D. S., Trigo, F.C., Martins, F.P.R., 2015, "Modelling, identification and a first control approach on the quality of flames in oil furnaces", Proceedings of the 8th International Conference on Integrated Modeling and Analysis in Applied Control and Automation (IMAACA 2015), Bergeggi, Italy, pp. 79-88.

Fleury, A.T., Trigo, F.C., Pacífico, A.L., Martins, F.P.R., 2018, "An inference model for combustion diagnostics in an experimental oil furnace", Expert Systems, Vol. 35, N. 2, pp. e12245, https://onlinelibrary.wiley.com/doi/abs/10.1111/exsy.12245.

Li, W., Chang, X., 2000. "Application of hybrid fuzzy logic proportional plus conventional integral-derivative controller to combustion control of stockerfired boilers", Fuzzy Sets and Systems, 111, pp. 267284.

González-Cencerrado, A., B. Peña, and A. Gil.,2012,"Coal flame characterization by means of digital image processing in a semi-industrial scale PF swirl burner." Applied energy, Vol. 94 , pp.375-384.

Mamdani, E.H. and S. Assilian, "An experiment in linguistic synthesis with a fuzzy logic controller", International Journal of Man-Machine Studies, Vol. 7, No. 1, pp. 1-13, 1975.

Prade, H., & Dubois, D., 1996, "What are fuzzy rules and how to use them", Fuzzy Sets and Systems, Vol.84, pp.169-185.

Silva, R.P., Fleury, A.T., Martins, F.P.R., Ponge-Ferreira, W.J.A., Trigo, F.C., 2015, "Identification of the state-space dynamics of oil flames through computer vision and modal techniques", Elsevier-Expert Systems with Applications, Vol. 42, N. 5, pp. 2421-2428.

Silva Neto, G. C., 2011, "Um Método para Solução de Problemas de Otimização Multiobjetivo em Ambiente Fuzzy". (Master's dissertation, PPGM- Federal University of Amazonas).

Sreedhanya, L. R., Varghese, A., Nair, M. S., & Wilscy, M., 2017, "Temperature mapping of a rotary kiln using fuzzy logic". Journal of Intelligent & Fuzzy Systems, Vol.32, N.4, pp.3059-3067.

Tóth, P., Garami, A., & Csordás, B. ,2017, "Image-based deep neural network prediction of the heat output of a step-grate biomass boiler". Applied energy, Vol.200, pp.155-169.

Zadeh, L.A., 1965, "Fuzzy sets", Information and control. , Vol. 8 N.3, pp. 338-353.

Zadeh, L.A., 1975, "The Concept of a Linguistic Variable and its Application to Approximate Reasoning-I", Information Sciences, Vol.8, pp.199-249.

RESPONSIBILITY NOTICE

The authors are the only responsible for the printed material included in this paper.